Journal of Engineering, Technology & Applied Science
p-ISSN: 2721-7949, e-ISSN: 2721-8090

Original Research Paper

Characteristics and Applications of Bionanosilica from Betung Bamboo Leaves

Esti Prihatini[1*], Gilang Dwi Laksono[1], Dhiya Khairunissa[2], Istie Rahayu[1], Rohmat Ismail[3]

[1] *Department of Forest Products, Faculty of Forestry and Environment, IPB University. Indonesia.*
[2] *Department of Chemistry, Faculty of Mathematics and Natural Sciences, Nusa Bangsa University. Indonesia.*
[3] *Department of Chemistry, Faculty of Mathematics and Natural Sciences, IPB University. Indonesia.*

Article History
Received:
28.10.2024

Revised:
19.11.2024

Accepted:
29.11.2024

***Corresponding Author:**
Esti Prihatini
Email:
esti@apps.ipb.ac.id

Abstract: Nanoparticles are materials that are currently widely used in research due to their novelty and the growing number of suitable applications. Silica nanoparticles can be produced by synthesizing using several methods such as melting, coprecipitation, sol-gel, and ultrasonication. The aim of this study is to determine the most appropriate synthesis method for the production of SiO_2 nanoparticles to optimize the quality of physical properties of fast-growing wood. The synthesis of SiO2 nanoparticles used in this study utilized three different methods: acid isolation method (F1), sol-gel method (F2), and reflux method (F3). Characterization of SiO2-NPs was performed using particle size analyzer (PSA), X-ray diffraction analysis (XRD), and Fourier transform infrared spectroscopy (FTIR). The results of PSA analysis showed that the acid isolation method produced the smallest SiO2 particle size compared to the sol-gel and reflux methods. The zeta pontential value in each method shows that the particles produced are unstable because the potential zeta value produced is around -10 mV to -30 mV. The results of FTIR and XRD analysis show that the synthesized material is a SiO_2 compound with a cristobalite phase. Application of the material on jabon wood through impregnation showed an improvement in physical properties, including an increase in WPG, density, and BE, especially in the sol-gel method (F2).

Keywords: Acid Isolation, Betung Bamboo Leaves, Bionanosilica, Jabon Wood Impregnation, SiO2 Nanoparticles.

Journal of Engineering, Technology & Applied Science, vol. 6, no. 3, pp. 153-166, December 2024. **DOI: 10.36079/lamintang.jetas-0603.766**

1. Introduction

Nanotechnology is a field of active research due to its novelty and growing applications [1]. Nanotechnology employs the characteristics of molecules or atomic structures with a diameter of approximately one billionth of a meter, or nanoparticles. Nanoparticles are defined as nanotechnology products with a particle size of 1-100 nm, as outlined by [2] . Nanoparticles can be synthesized through the application of chemical and physical methods. Nanoparticles can be classified into two principal categories: organic and inorganic. Organic nanoparticles are composed of carbon-based materials, including cellulose and chitosan. In contrast, inorganic nanoparticles are formed from metals, such as Fe3O4 [3]. The extensive utilization of metal nanoparticles has facilitated advancements in a multitude of fields, including agriculture, catalysis, and biomedical engineering. Research on the use of nanoparticles has been conducted, including studies on the use of SiO_2 nanoparticles [4], TiO2 [5] [6] and Fe3O4 [7].

Silica nanoparticles possess advantageous characteristics, including a large surface area and good heat resistance [8]. Consequently, they can be utilized as adsorbents and catalyst components [9]. Silica nanoparticles can be synthesized via a number of methods, including melting, coprecipitation, sol-gel, calcination, and ultrasonication. In this study we used 3 methods in the synthesis of silica namely sol-gel method, acid isolation method and reflux method. The sol-gel method offers several advantages such as a relatively easy process, using low temperatures during the process, relatively low cost, producing products with high purity and uniformity and non-toxic [10]. The extraction of silica from bamboo leaves using the sol-gel method has been shown to reach 87.02% [11]. As reported by [12], alternative techniques such as acid isolation have produced biosilica with a purity level of 96%. The use of these extractive methods in relation to acid leaching time, acid concentration, and extraction time and temperature has a significant impact on the quality of the biosilica produced. Extending the extraction time leads to an increase in biosilica purity. In addition to the two methods described in the previous sentence, there is also a coprecipitation method that offers the advantages of high purity, a simple precipitation process that facilitates separation at low temperatures, relatively fast time, the simplest method and easy to perform [13].

The use of SiO_2 nanoparticles as an impregnation material has been demonstrated to enhance the strength and quality of fast-growing wood species, including jabon [14]. It is postulated that this phenomenon is due to the even distribution and penetration of nanoparticles within the wood [15]. The findings of previous research indicate that impregnating sengon wood with monoethylene glycol (MEG) and SiO_2 nanoparticles can effectively enhance the quality of the wood [4]. As stated by [14], impregnation of poplar wood (Populus spp.) with furfuryl alcohol (FA) and nano SiO_2 has been demonstrated to effectively enhance the quality of the wood. Wood impregnation can be classified into three main categories: diffusion, capillary, and pressure treatment [16]. Wood impregnation is one of the modifications of wood by introducing chemicals into the wood to be deposited in the wood without damaging the wood [17]. In addition, according to [18], stated that in the impregnation process there will be a chemical reaction with the most effective groups in the wood cell wall. The utilisation of metal nanoparticle-impregnated wood can enhance the durability of the wood and other properties of the wood. The synthesis method employed for silica nanoparticles can influence the characteristics of the resulting nanoparticles, including their size, shape, and size distribution [19]. Accordingly, the present study compares the synthesis of SiO_2 nanoparticles via three methods: acid isolation, sol-gel, and reflux. These methods were selected due to their compatibility with jabon wood. The objective of this study is to ascertain the most appropriate synthesis method for the production of SiO_2 nanoparticles, with a view to optimising the quality of the physical properties of fast-growing wood.

2. Literature Review

2.1. Wood Modification

Wood modification represents a promising avenue for enhancing the quality of fast-growing wood. As stated by [20], wood modification processes are employed to enhance the physical, mechanical, or aesthetic attributes of wood. The objective of wood modification is to achieve enhanced performance, including improved dimensional stability, resistance to decay, and resistance to weathering, among other benefits [21]. A variety of wood modification techniques exist, including impregnation modification, wood biotechnology modification [22], wood chemical modification [23], and wood thermal modification [24].

Journal of Engineering, Technology & Applied Science, vol. 6, no. 3, pp. 153-166, December 2024. **DOI: 10.36079/lamintang.jetas-0603.766**

Wood modification can be classified into two main categories: active and passive. Active modification refers to processes that result in natural chemical changes in the material, whereas passive modification involves changes in the properties of the material without altering its chemical composition. Impregnation modification is an example of a passive modification technique. The chemical modification of wood necessitates a site where chemical reactions of the agent occur with the polymeric constituents of the wood (lignin, hemicellulose, or cellulose), thereby resulting in the formation of stable covalent bonds between the reagent and the cell wall polymers [25]. In this instance, the chemical modification of wood is regarded as an active modification, given that it gives rise to chemical alterations to the cell wall polymer. Wood impregnation is one of the methods of wood modification that aims to alter the properties of wood by modifying the cell wall level using chemicals or a combination of chemicals. This process facilitates the formation of a bulking agent [17]. Impregnation modification is a passive modification process, whereby although the properties of the wood are affected during the modification treatment, no chemical change occurs. This passive modification entails the impregnation of the cell wall with monomers, which are subsequently polymerized in situ to fill the cell wall and lumen.

2.2. Jabon Wood

Jabon wood (Anthocephalus cadamba) is a fast-growing wood native to South and Southeast Asia, including Indonesia [26]. Jabon wood is a softwood with a number of beneficial properties, including suitability as a raw material for plywood, use in lightweight construction, and other applications. The wood texture of jabon is slightly fine to slightly rough, with straight fibrous characteristics, a lack of gloss, and an odorless quality. Jabon wood has a specific gravity of approximately 0.42 (0.29-0.56), including Strength Class III-IV and Durability Class V. Its pores are radially multiple and diffuse, consisting of 2-3 pores with a diameter of 130-220 μm and a frequency of 2-5 per mm² with simple perforation planes [27].

2.3. Silicon Dioxide Nanoparticle

Silica (SiO_2) can be obtained from inorganic materials, including sand, clay, and rocks. In contrast, silica derived from organic materials can be obtained from sources such as corncob ash, palm fronds, and bamboo. Silica can be comprised of silanol groups (Si-OH), siloxane bridges (Si-O-Si), and hydrogen-bonded water, which can be identified on the surface or within amorphous internal structures [28]. Nano-SiO_2 is a white powder comprising amorphous silica with an exceptionally high degree of purity. Nano-SiO_2 is defined as a single particle of silica dioxide, an inorganic metal oxide, with a diameter of less than 100 nm [4]. Nano-SiO_2 exhibits several advantageous properties, including a large specific surface area, strong surface adsorption, high surface energy, and high chemical purity and dispersion. These properties are attributed to the nano-SiO_2 having a small particle size [29]. Nanosilica is employed in a multitude of applications, including its use as a catalyst precursor, an absorbent, and a component of composite filters [30].

Nano-SiO_2 in amorphous form is non-toxic and capable of interacting with biological environments [31]. Furthermore, Nano-SiO2 is one of the most appealing nanoparticles due to its numerous advantageous characteristics, including a relatively low cost, non-toxic properties, biocompatibility, and high heat resistance [32]. However, the high hydrophilicity of the nano-SiO2 surface can result in the formation of agglomerates and difficulties in dispersion within the polymer matrix. As stated by [33], nano-SiO2, which has a low viscosity, can be more readily distributed in wood. The incorporation of nano-SiO_2 into wood as a polymer enhances the strength and optimizes the intrinsic characteristics of wood [14], while augmenting its resilience to UV radiation, fire, and moisture.

2.4. Wood chemistry

The chemical components of wood can be classified into two principal categories: structural components and extractive components. The structural components constitute the cell wall structure and are accountable for cell shape, including cellulose, hemicellulose, and lignin (see Figures 1 and 2). Extractive components are non-structural components present within cell lumina, cellular cavities, or channels. These components can be extracted using solvents with adequate polarity without any alteration to their cellular structural characteristics. The inorganic component constitutes part of the extractive component, representing a percentage of less than 1%. It is often referred to as ash [34].

Figure 1 showing anhydrous glucose monomer units derived from β-D-glucopyranose, inter-monomeric 1-4 glycosidic linkages, and structural linkages of cellobiose units [34].

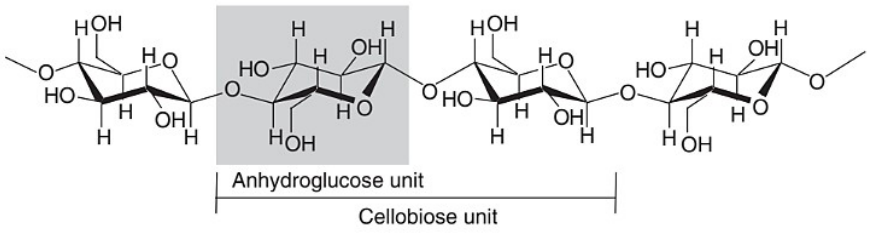

Figure 1. Presentation of Cellulose Molecules

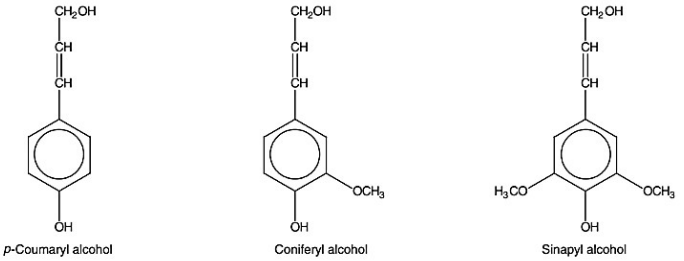

Figure 2. Chemical Structure of Lignin Constituent Monomers in Wood [34]

3. Methodology

3.1. Materials

Samples of jabon wood, which has reached the age of five and is free of defects, were obtained from community forests situated within the Bogor region of West Java. The jabon wood specimens exhibited a height of 7-9 meters with a diameter at breast height of 25-28 cm, exhibiting a branch-free growth pattern. Subsequently, the wood was cut to a length of 50 cm from the base to the limit of the branch-free height. All samples were derived from a single tree and processed concurrently to ensure minimal variability in properties. The chemical agents employed in this process include betung bamboo leaves, 37% hydrochloric acid (Merck), sodium hydroxide (Merck), ammonium hydroxide (Merck), sulfuric acid (98%) (Merck), ethanol, and demineralized water.

3.2. Methods

1) Preparation of Test Sample

Fast-growing wood was sampled by cutting it using a chainsaw and table saw without distinguishing between sapwood and heartwood. A total of 30 test samples, each measuring 2 cm x 2 cm x 2 cm, were prepared, with 10 replicates of the physical properties test. Subsequently, the samples were subjected to a physical properties test, with parameters of weight percent gain (WPG), bulking effect (BE), and density.

2) Charring of Betung Bamboo Leaves

One hundred grams of betung bamboo leaves were subjected to a cleaning process involving the use of running water. They were then subjected to an oven-drying process at a temperature of 105°C for a period of three hours. Following this, the leaves were burned in a burner at a temperature of 550°C for a period of two hours, resulting in the formation of charcoal [9]. Subsequently, the resulting charcoal was pulverized and filtered through a 100-mesh sieve. The subsequent phase entails the heating of 50 grams of charcoal powder in a furnace at 700°C for a period of two hours, until the complete formation of ash [35].

3) Synthesis of SiO_2 Nanoparticles by Acid Isolation Method

The nano silica isolation process commences with the mixing of 1 gram of betung bamboo leaf ash with 10 mL of 1 M HCl. The resulting mixture is then stirred with a stirrer for a period of 2 hours at

3000 rpm [12]. Subsequently, the mixture was subjected to centrifugation at 5000 rpm for 15 minutes, after which the supernatant was discarded. The precipitate, in the form of white crystals, was then washed with hot water until the pH was neutralized. It was subsequently dried at 105°C for three hours and then calcined at 450°C for three hours.

4) Synthesis of SiO_2 Nanoparticles by Sol-Gel Method

A total of 1 gram of ash derived from betung bamboo leaves was added to 40 ml of 3M HCl solution. The mixture was then stirred while being heated at 80°C for one hour with a hotplate stirrer. Following the completion of the aforementioned process, the mixture was permitted to cool and subsequently filtered, whereby the precipitate phase was extracted. The resulting precipitate was then added to 40 mL of 3 M NaOH, and the mixture was stirred while heated at 90°C for one hour [36]. Subsequently, the mixture was allowed to cool and filtered, resulting in the collection of the liquid phase. The separated liquid phase was combined with 40 mL of distilled water and 20 mL of 96% ethanol, then stirred until homogeneous. Subsequently, 3 M HCl was added slowly until the pH reached a neutral level, forming a white precipitate with a sol-gel system [37]. The resulting white precipitate was filtered and dried at 105°C for two hours and subsequently calcined at 450°C for three hours [38].

5) Synthesis of SiO_2 Nanoparticles by Reflux Method

Ten grams of furnace ash were refluxed in 80 milliliters of 3 N NaOH for three hours. Subsequently, the solution was filtered using filter paper, and the residue was washed with 50 mL of boiling distilled water. The filtrate was then cooled to room temperature. Subsequently, the filtrate was titrated with 5 N H_2SO_4 until the pH reached 2, followed by the addition of 2.5 N NH_4OH until the pH reached 8.5. The aforementioned process was conducted using magnetic stirrer equipment. The filtrate solution was then left at room temperature for 30 minutes, after which rinsing was conducted using demin water until the solution reached neutral pH. The solution was then dried at 105°C for 12 hours [39].

6) Impregnation Process on Wood

The impregnation process was conducted on samples that had not undergone any prior treatment, as well as on samples that had been impregnated with a mixture of SiO_2 nanoparticles. This mixture was synthesized using three distinct methods, with a concentration of 5% by volume. Subsequently, the prepared solution was agitated using a Cole-Parmer brand sonicator with an amplitude of 40% for a period of 60 minutes. Prior to commencing the impregnation process, the wood samples were subjected to oven drying at 105°C for a period of 48 hours. The mixture should then be poured into a container that has already been filled with the wood samples. Finally, nylon wire weights should be added, ensuring that they do not come into contact with the impregnation solution. The container should then be placed within the impregnation tube. The impregnation process was conducted under a vacuum of -0.5 bar for 30 minutes, followed by a 120-minute period under a pressure of 1 bar. Once the impregnation process is complete, the wood is rinsed with demineralized water in order to remove any residual impregnation solution. Subsequently, the wood was wrapped in aluminum foil and heated at 65°C for 12 hours, then dried in an oven at 105°C for 48 hours until the weight remained constant. It is necessary to measure the mass and dimensions of the wood in order to calculate the percentage of water in the grain (WPG), the density, and the percentage of bulking effect (BE).

7) Physical Properties Evaluation

The weight percent gain (WPG) was calculated using the following formula (Equation1):

$$WPG\ (\%) = \frac{W_1 - W_0}{W_0}\ x\ 100 \tag{1}$$

W_0 represents the oven-dry weight of the sample prior to impregnation, whereas W_1 denotes the oven-dry weight of the sample following impregnation.

The Bulking Effect (BE) test was calculated using the following formula (Equation 2):

Journal of Engineering, Technology & Applied Science, vol. 6, no. 3, pp. 153-166, December 2024. **DOI: 10.36079/lamintang.jetas-0603.766**

$$SE\ (\%) = \frac{V_1 - V_0}{V_0}\ x\ 100 \tag{2}$$

V_0 represents the volume of the sample prior to impregnation (cm^3), whereas V_1 denotes the volume of the sample following impregnation (cm^3).

The density (ρ) was calculated before and after the treatment using the following formula (Equation 3):

$$\rho\ ((kg/m^3) = \frac{W_1}{V_1} \tag{3}$$

3.3. Characterization of SiO_2 Nanoparticles

1) Fourier Transform Infrared Spectrometry

The sample was mixed with potassium bromide (KBr) in a ratio of 1:100, forming pellets. The pellets were subjected to analysis by Fourier Transform Infrared Spectrometry (FTIR) (Nicolet 6700 Thermo Scientific, USA), with scanning conducted across the range of 4000 to 400 cm-1 at a resolution of 4 cm-1 for 32 scans.

2) Particle Size Analyzer

A total of 10 mg of SiO_2 nanoparticles synthesized using three methods were dissolved in 100 mL of demineralized water and then stirred for 15 minutes with a sonicator [40]. The solution, containing 100 ppm of SiO_2 nanoparticles, was subjected to analysis using a Particle Size Analyzer (PSA) Beckman Coulter LS 13 320 XR) to determine the particle size distribution.

3) X-Ray Diffraction Analysis

The synthesized SiO_2 nanoparticles were also subjected to X-ray diffraction (XRD) analysis. One gram of SiO_2 nano powder, sieved to pass 100 mesh, was obtained. The degree of crystallinity of the SiO_2 nano powder was analyzed by XRD-PANAnalytical Empyrean type with PIXcel 1D detector. The device was operated with the following parameters: Cu Kα radiation with a graphite monochromator, 40 kV voltage, 30 mA current, and a 2θ scan range between 5° and 70° with a scan speed of 2°/minute. The data were processed using Origin 8.5 software (Northampton, MA, USA) for the spectra and diffractograms. The elucidation of inorganic molecules was conducted using QualX software (Rome, Italy) and Vesta software (Ibaraki, Japan).

4) Data Processing

This study employed a completely randomized design (CRD) and was evaluated using analysis of variance (ANOVA), followed by Duncan's post hoc test at α = 5%. The tests were conducted using the IBM SPSS Statistics software, version 25.0, which is a statistical package designed for use with the Social Sciences. The data obtained from the FTIR characterization of SiO_2 nanoparticles were processed using the Origin program, version 8.5.

4. Finding and Discussion

4.1. Characterization of Silica Dioxide Nanoparticles

The FTIR spectrum in Figure 3 was subjected to analysis to identify the functional groups present in the synthesized biosilica (SiO2) sample. The results of the analysis of the Silica Dioxide Nanoparticles (SiO2-NPs) sample by reflux method identified a peak at wave number 797 cm-1, which is the Si-O functional group, and a peak at wave number 1104 cm-1, which is the Si-O-Si functional group. As demonstrated in reference [4], a peak at 1056 cm-1 was also detected, which is the peak of silica Si-O-Si vibrations. The presence of the Si-O-Si functional group is indicative of the presence of silica content. This finding aligns with the conclusions of [41], who proposed that the wave number range of 1050-1115 cm-1, which corresponds to the vibration of Si-O-Si, is indicative of the presence of silica.

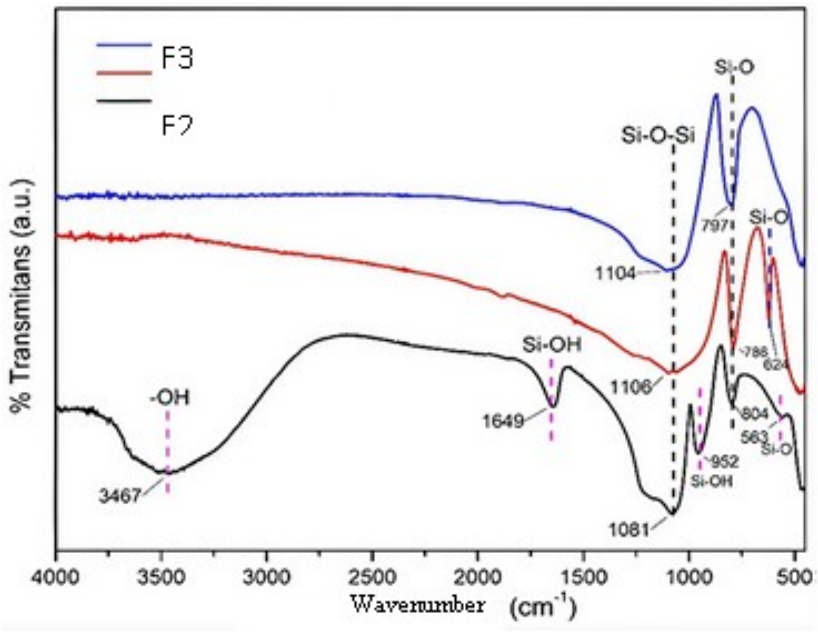

F1: Acid isolation, F2: Sol-Gel, and F3: Reflux

Figure 3. FTIR was Employed to Analyze the Samples Using Three Different Methods

The results of the sol-gel method sample analysis identified the functional groups of Si-O at 786 cm-1 and 624 cm-1. The functional group of Si-O-Si was identified at a wave number of 1106 cm-1. Additionally, research conducted by [42] indicated the presence of Si-O-Si functional groups at a wave number of 1100 cm-1, as observed in the sol-gel method of silica extraction. The results of the sample analysis of the acid isolation method identified the functional groups of Si-O at wave numbers 804 cm-1 and 563 cm-1. The functional group of Si-O-Si was identified at a wave number of 1081 cm-1. The functional groups of Si-OH were identified at wave numbers 1649 cm-1 and 952 cm-1, as well as at 3476 cm-1, which corresponds to the OH functional group. The presence of OH functional groups can be attributed to the presence of acidic residues that exhibit hygroscopic properties. The findings of the study conducted by [43] also indicated the presence of silanol and hydroxy groups, which were attributed to the adsorption of water molecules on the silica surface. These groups were identified at wave numbers 3750 cm-1 and 2800 cm-1, respectively. The results of this FTIR analysis demonstrate that the compounds synthesized from betung bamboo leaves by the three methods are indeed silica. This is evidenced by the identification of functional groups within the silica framework, namely silanol (Si-OH) and siloxane (Si-O-Si).

The analysis of particle size is a factor in the efficiency of wood impregnation. It has been demonstrated that particles of a smaller size are more effective at penetrating the wood. The study by [44] demonstrated that particle sizes of 70 nm can be impregnated with greater efficiency than those of 170 nm. The deployment of particle size analysis instruments in nanotechnology applications is of paramount importance with respect to efficiency, stability, and quality control [45].

Figure 4 shows the results of the PSA analysis for the aforementioned methods, while Figure 5 shows the results of the zeta potential analysis for the three methods.

The mean particle size of nanosilica produced via the acid isolation method was determined to be 120 nm. The mean particle size of silica in the range of 5-20 microns was produced in rice husk ash using the extraction method [12]. The average particle size of nanosilica produced using the sol-gel method was 207 nm. This result is smaller than that reported by [42], who observed a particle size of 315 nm for silica produced via the sol-gel method. The average size of the nanosilica particles produced using the reflux method was found to be 230 nm (Figure 4). This result is greater than that reported by [46], who produced nanosilica with a particle size of 93 nm.

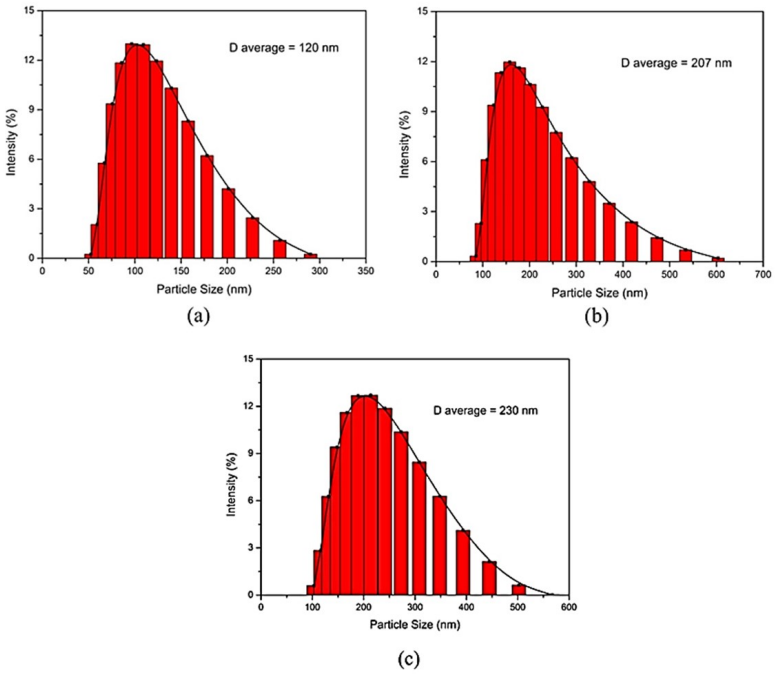

Figure 4. PSA Analysis for the Aforementioned Methods are as Follows: (a) Acid Isolation, (b) Sol-Gel, and (c) Reflux.

The zeta potential results for nanosilica obtained using the acid isolation method exhibited an average value of -12.43 mV (Figure 5). As demonstrated by [47], the zeta potential of SiO2 is negative, with a value of -25.8 mV. The resulting nanosilica exhibits a zeta potential of less than 30 mV, indicating its capacity for facile dispersion in the form of a dispersed solution [48]. These negative zeta potential results are consistent with the existing literature, which reports values ranging from -10 mV to -50 mV [49], indicating that the surface is negatively charged.

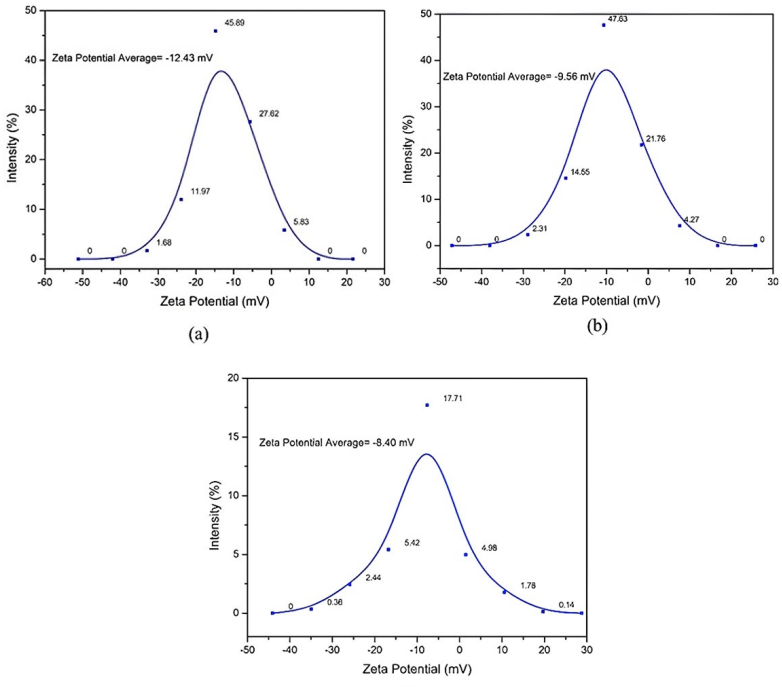

Figure 5. Zeta Potential Analysis for the Three Methods: (a) Acid Isolation, (b) Sol-Gel, and (c) Reflux.

The negative zeta potential is the result of the dissociation of Si-O or silanol groups on the nanosilica surface, which leads to the formation of negative zeta potential of siloxane (Si-O-Si) groups [50]. The zeta potential analysis of nanosilica using the sol-gel method yielded an average value of -9.56 mV, while the reflux method produced an average value of -8.40 mV. The zeta potential value for nanosilica in all three methods is below -20 mV, indicating incipient stability behavior [51]. The presence of van der Waals forces, which are responsible for stronger inter-particle attraction, is indicated by low zeta potential values, resulting in the flocculation of particles [52].

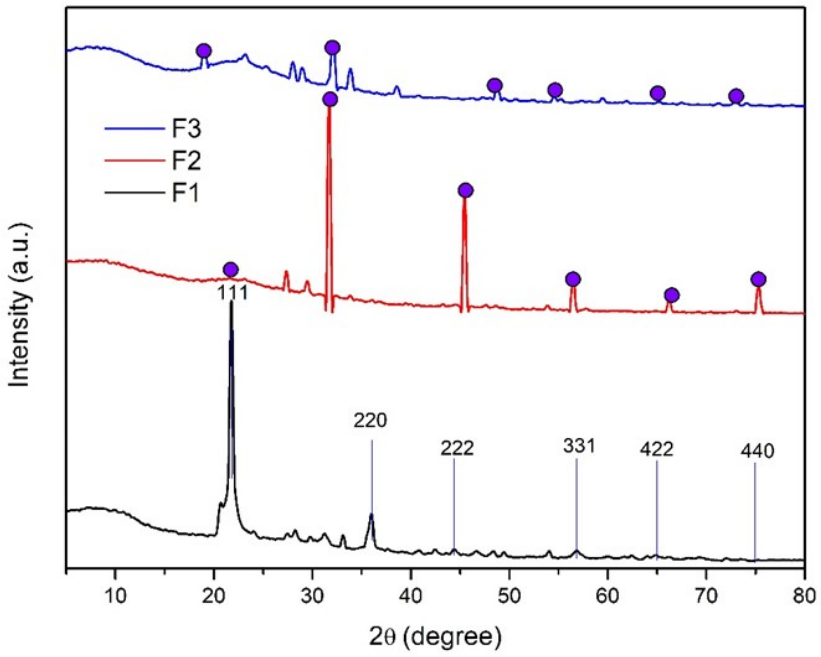

Figure 6. Difractogram of the Synthesized Bionanosilica

X-ray diffraction (XRD) analysis was employed to ascertain the phase, crystallinity degree, and crystal size of the synthesized bionanosilica. The diffractogram of the bionanosilica sample (Figure 6) exhibited peaks at 2θ values of 21.83, 35.90, 44.39, 56.93, 64.96, and 75.02° for the F1 method, peaks at 2θ values of 21.74, 34.70, 45.37, 56.62, 65.08, and 75.36° for the F2 method, and peaks at 2θ values of 21.07, 34.81, 45.27, 56.10, 64.87, and 74.47° for the F3 method. The data were analyzed by comparing the standard cristobalite diffractogram, namely JCPDS card number 04-008-7642 [53], and it was confirmed that these peaks are silica compounds with a cristobalite phase.

Table 1. Crystallinity Degree and Crystal Size Values of the Bionanosilica

No	Method	Degree of crystalinity (%)	Crystal size (nm)
1	F1	25.37	8.04
2	F2	20.74	10.80
3	F3	14.48	20.41

The degree of crystallinity of bionanosilica is determined by calculating the ratio between the area of the crystalline lattice and the total number of lattices (amorphous and crystalline). The degree of crystallinity of bionanosilica, as calculated using the F1, F2, and F3 methods, yielded values of 25.37%, 20.74%, and 14.48%, respectively (Table 1). The degree of crystallinity of bio-nanosilica can influence its characteristics, including mechanical strength, thermal stability, and reactivity as a

Journal of Engineering, Technology & Applied Science, vol. 6, no. 3, pp. 153-166, December 2024. **DOI: 10.36079/lamintang.jetas-0603.766**

catalyst [54]. An increase in crystallinity can enhance these properties, thereby rendering nanoparticles more efficacious in their applications [55]. The dimensions of bionanosilica crystals are determined through the application of the Scherrer equation (eq.4), which employs the following variables: λ, the wavelength of the X-rays utilized; θ, the diffraction angle; and K, a constant whose value is contingent upon the crystal form factor, the diffraction plane (hkl), and the definition of the β value utilized as the full width at half maximum (FWHM) or integral width of the peak [56].

$$D = \frac{K\lambda}{\beta \cos\theta} \tag{4}$$

The results of Scherrer equation calculations show that the crystal size of bionanosilica with F1 method is 8.04 nm, F2 method is 10.80 nm, and F3 method is 20.41 nm. These results indicate that the type of synthesis method affects the size of the crystals produced. The crystal size of nanoparticles can significantly affect their properties, namely their surface area and melting point. Smaller nanoparticles have a higher surface area to volume ratio, which can improve their reactivity and catalytic properties. In addition, as particle size decreases, the melting point can also decrease due to a higher percentage of surface atoms [57].

The F1 and F2 methods exhibit a lower degree of crystallinity and a larger crystallinity size than F1. This phenomenon can be attributed to the sol-gel nature of both F1 and F2, which inherently possess the potential for agglomeration. In the absence of adequate control, the synthesis of nanoparticles via the sol-gel method can result in the agglomeration of particles, leading to a lack of uniformity in size, shape, and degree of crystallinity [58]. Moreover, the F3 method, when combined with the ultrasonication process, results in the lowest degree of crystallinity. This phenomenon can be attributed to the formation of cavitation (air bubbles that form and burst) from the ultrasonic waves, intense local heating, and mechanical stress, which can disrupt the ordered crystal structure [59]. These effects are not observed in the F1 method, which employs a simpler acid isolation process, resulting in the highest degree of crystallinity and the smallest crystal size.

Figure 7 shows the crystal structure of bionanosilica is illustrated in two forms: a polyhedron crystal and a two-dimensional ball-stick pattern in a tetragonal crystal structure. In this context, the notations a, b, c,and o represent a three-dimensional coordinate system with an origin (o) and three mutually perpendicular coordinate axes: the x-axis (a), the y-axis (b), and the z-axis (c).

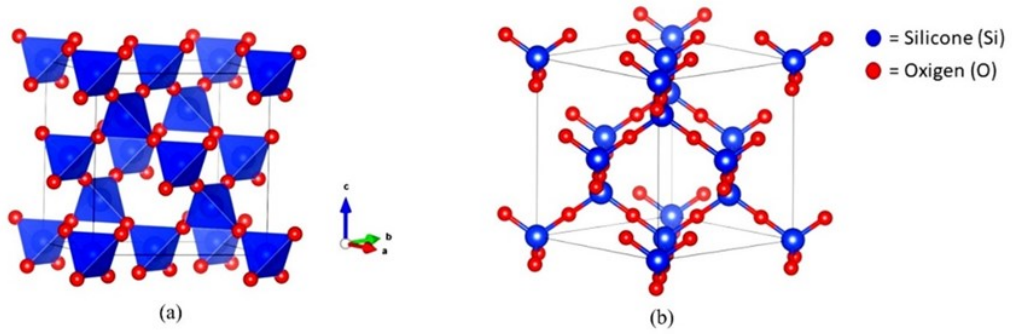

Figure 7. The Crystal Structure of Bionanosilica

A thorough understanding of the crystal structure is crucial for comprehending the material's physical properties and chemical reactions. An understanding of the arrangement of atoms can facilitate the prediction and explanation of the physical properties of materials, including factors such as melting point, hardness, and conductivity. Furthermore, knowledge of the crystal structure enables the prediction of a material's reaction with other substances, which is a crucial aspect of the material synthesis process [60]. The crystal structure of bionanosilica was determined through the elucidation of its crystal diffractogram pattern with QualX software from [61], and then continued with visualization using Vesta software. The analysis demonstrated that the bionanosilica under

investigation exhibits a cristobalite phase with a tetragonal crystal structure (Figure 7). This result is consistent with the assertion of [62] that silica compounds with a cristobalite phase possess a tetragonal crystal structure in class 4 2 2 - trapezohedral with space group P41 21 2 and cell parameters a = 4.9709 Å, c = 6.9278 Å.

4.2. Physical Properties Testing of SiO_2-NPs Impregnated Jabon Wood

The dimensional stability parameter, defined as the addition of weight to a wood sample expressed as a percentage, is a measure of the degree of treatment. This value is referred to as the weight percent gain (WPG). An elevated WPG value suggests that a greater quantity of polymers are introduced into the wood following the treatment process. Table 2 illustrates the WPG values of jabon wood impregnated with NP-SiO_2 particles using three distinct methods.

Table 2. Presents the Results of the Physical Property Measurements of Impregnated Jabon Wood

No	Method	WPG (%)	BE (%)	Density (g/cm^3)
1	Untreated	1.09 ± 0.45	2.14 ± 0.19	0.34 ± 0.06
2	F1	-3.59 ± 0.59	13.68 ± 0.24	0.36 ± 0.01
3	F2	1.10 ± 0.42	13.94 ± 0.14	0.38 ± 0.01
4	F3	-0.15 ± 0.42	13.81 ± 0.41	0.37 ± 0.01

The highest WPG value of 1.1% was observed for jabon wood impregnated with SiO2-NPs synthesized by the sol-gel method, while the second highest value of -0.15% was observed for the reflux method. The lowest WPG value of -3.59% was observed for the acid isolation method. The data in the aforementioned table demonstrate that SiO2-NPs synthesized via the sol-gel method were successfully incorporated and filled the wood cavity to a greater extent than those produced by the reflux and acid isolation methods. The sol-gel method for synthesizing silica not only produces a high WPG value but also yields the highest Bulking Effect (BE) and density values compared to the acid isolation and reflux methods. The BE and density values for the sol-gel method are 13.94% and 0.38 (g/cm³), respectively. The lowest value for both the BE and density parameters is observed for jabon wood impregnated SiO2-NPs using the acid isolation method, with a value of 13.68% and 0.36 (g/cm³), respectively. As posited by [17], a higher BE value signifies a greater degree of polymer filling within the wood cavity. Consequently, jabon wood impregnated SiO2-NPs, synthesized via the sol-gel method, exhibits a superior capacity to resist dimensional contraction and wood development. As indicated by the density value, as cited by [63], an elevated density value is indicative of thicker cell walls in the wood. This can be attributed to the presence of nanoparticles, which effectively fill the wood cavity through the impregnation process [64].

5. Conclusion

The results of analytical testing conducted using FTIR, PSA, and XRD, show that SiO_2-NPs have been successfully synthesized through the application of the three methods used in this study. The acid isolation method proved to be the most effective for synthesizing SiO2-NPs from betung bamboo leaves compared to the sol-gel and reflux methods, producing the smallest particle size and highest level of crystallinity. zeta potential results show that the three methods used produce unstable particles because the values are around -10 mV to - 30 mV. Judging from the value of the physical properties of wood during the impregnation process, the sol-gel synthesis method produced higher values of WPG, BE and density, indicating that nano silica was successfully dispersed into jabon wood. These results not only aid in comprehending the synthesis of SiO_2-NPs from natural biomass sources but also establish a basis for future studies focused on enhancing these techniques for large-scale manufacturing. The small particle size and high crystallinity of these SiO_2 nanoparticles make them ideal for use in drug delivery, catalysis, and environmental remediation. The sol-gel technique may be suitable for jabon wood, creating customized SiO_2 NPs for industrial applications. Future research should prioritize scalability and investigate the environmental and cost implications of using agricultural and forestry byproducts for nanoparticle synthesis. Additional examination of the functional characteristics of the synthesized SiO_2 NPs is essential for their commercialization.

Acknowledgement
We would like to express my gratitude to the Department of Forest Products for providing the necessary research facilities and to the Directorate of Human Resources of IPB University for offering financial support for this research project through the Functional Position Grant Year 2024, contract No. 08/Hibahkom/IPB/2024.

References

[1] S. Khan *et al.*, "A review on nanotechnology: Properties, applications, and mechanistic insights of cellular uptake mechanisms," *J. Mol. Liq.*, vol. 348, p. 118008, 2022.
[2] S. Khan and M. K. Hossain, "2 - Classification and properties of nanoparticles," in *Woodhead Publishing Series in Composites Science and Engineering*, S. Mavinkere Rangappa, J. Parameswaranpillai, T. G. Yashas Gowda, S. Siengchin, and M. O. B. T.-N.-B. P. C. Seydibeyoglu, Eds., Woodhead Publishing, 2022, pp. 15–54.
[3] P. Kumar, F. Gonelimali, M. Máté, and P. Sharma, "Characteristics, Composition, and Structure of Organic Nanomaterials BT - Organic-Based Nanomaterials in Food Packaging," K. Younis, O. Yousuf, and S. Ul Islam, Eds., Cham: Springer Nature Switzerland, 2024, pp. 15–34.
[4] F. C. Dirna, I. Rahayu, L. H. Zaini, W. Darmawan, and E. Prihatini, "Improvement of fast-growing wood species characteristics by MEG and nano SiO2 impregnation," *J. Korean Wood Sci. Technol.*, vol. 48, no. 1, pp. 41–49, 2020.
[5] I. Rahayu, W. Darmawan, D. S. Nawawi, E. Prihatini, R. Ismail, and G. D. Laksono, "Physical Properties of Fast-Growing Wood-Polymer Nano Composite Synthesized through TiO2 Nanoparticle Impregnation," *Polymers*, vol. 14, no. 20. 2022.
[6] E. Prihatini, R. Ismail, I. S. Rahayu, G. D. Laksono, and D. Khairunissa, "Compatibility Testing of Synthesized TiO2 Nanoparticles on The Fast-Growing Wood Physical Properties," *J. SAINS Nat.*, vol. 14, no. 2, pp. 62–73, 2024.
[7] S. L. Fadia, I. S. Rahayu, D. S. Nawawi, R. Ismail, and E. Prihatini, "The Physical and Magnetic Properties of Sengon (Falcataria moluccana Miq.) Impregnated with Synthesized Magnetite Nanoparticles," *J. Sylva Lestari*, vol. 11, no. 3, pp. 408–426, 2023.
[8] B. McLean and I. Yarovsky, "Structure, Properties, and Applications of Silica Nanoparticles: Recent Theoretical Modeling Advances, Challenges, and Future Directions," *Small*, vol. n/a, no. n/a, p. 2405299, Oct. 2024.
[9] P. U. Nzereogu, A. D. Omah, F. I. Ezema, E. I. Iwuoha, and A. C. Nwanya, "Silica extraction from rice husk: Comprehensive review and applications," *Hybrid Adv.*, vol. 4, p. 100111, 2023.
[10] L. P. Singh *et al.*, "Sol-Gel processing of silica nanoparticles and their applications," *Adv. Colloid Interface Sci.*, vol. 214, pp. 17–37, 2014.
[11] Z. A. Rizky, A. A., Muhammad, M., Ginting, Z., Nurlaila, R., & Nasrul, "Pengaruh Variasi Suhu Dan Lama Waktu Pembakaran Terhadap Hasil Sintesis Silika Dari Daun Bambu Menggunakan Metode Sol-Gel," *Chem. Eng. J. Storage (CEJS), 2(5)*, pp. 107–116, 2023.
[12] S. Steven, E. Restiawaty, and Y. Bindar, "Operating Variables on Production of High Purity Biosilica from Rice Hull Ash by Extraction Process.," *J. Eng. Technol. Sci.*, vol. 54, no. 3, 2022.
[13] J. Y. Park, Y. M. Gu, J. Chun, B.-I. Sang, and J. H. Lee, "Pilot-scale continuous biogenic silica extraction from rice husk by one-pot alkali hydrothermal treatment and ball milling," *Chem. Biol. Technol. Agric.*, vol. 10, no. 1, p. 102, 2023.
[14] Y. Dong, Y. Yan, S. Zhang, and J. Li, "Wood/Polymer Nanocomposites Prepared by Impregnation with Furfuryl Alcohol and Nano-SiO2," *BioResources*, vol. 9, Aug. 2014.
[15] M. Bak, Z. Plesér, and R. Németh, "Improving the Decay Resistance of Wood through the Fixation of Different Nanoparticles Using Silica Aerogel.," *Gels (Basel, Switzerland)*, vol. 10, no. 4, Apr. 2024.
[16] W. Bi *et al.*, "Effects of chemical modification and nanotechnology on wood properties," *Nanotechnol. Rev.*, vol. 10, pp. 978–1008, Aug. 2021.
[17] C. Hill, *Wood Modification. Chemical, Thermal and Other Processes.* London: John Wiley & Sons, 2006.
[18] A. M. C. Yona, J. Žigon, P. Matjaž, and M. Petrič, *Potentials of silicate-based formulations for wood protection and improvement of mechanical properties: A review*, vol. 55, no. 4. 2021.
[19] J. K. Patra and K. Baek, "Green Nanobiotechnology : Factors Affecting Synthesis and

Characterization Techniques," vol. 2014, 2014.
[20] D. Sandberg, A. Kutnar, and G. Mantanis, "Wood modification technologies - A review," *iForest - Biogeosciences For.*, vol. 10, pp. 895–908, Dec. 2017.
[21] C. Hill, "Wood modification: An update," *Bioresources*, pp. 918–919, 2011.
[22] R. Hartono, Erwinsyah, W. Hidayat, and R. Damayanti, "Effect of impregnation methods and bioresin concentration on physical and mechanical properties of soft-inner part of oil palm trunk," *J. Phys. Conf. Ser.*, vol. 1282, no. 1, 2019.
[23] P. Gérardin, "New alternatives for wood preservation based on thermal and chemical modification of wood— a review," *Ann. For. Sci.*, vol. 73, no. 3, pp. 559–570, 2016.
[24] W. Hidayat and F. Febrianto, *Teknologi Modifikasi Kayu Ramah Lingkungan: Modifikasi Panas dan Pengaruhnya terhadap Sifat-sifat Kayu*. Bandar Lampung: Pusaka Media, 2018.
[25] R. Rowell, *Wood Chemistry and Wood Composites*. United States: CRC Press, 2012.
[26] H. Krisnawati, M. Kallio, and M. Kanninen, *Anthocephalus cadamba Miq.: ekologi, silvikultur dan produktivitas*. 2011.
[27] A. Martawijaya, I. Kartasujana, K. Kadir, and S. Prawira Among, "Atlas Kayu Indonesia Jilid 1." Departemen Kehutanan. Badan Penelitian Dan PengembanganKehutanan, Bogor (ID), pp. 1–171, 2005.
[28] M. Kosmulski and M. Kalbarczyk, "Zeta Potential of Nanosilica in 50% Aqueous Ethylene Glycol and in 50% Aqueous Propylene Glycol," *Molecules*, vol. 28, no. 3. 2023.
[29] C. Zhuang and Y. Chen, "The effect of nano-SiO2 on concrete properties: A review," *Nanotechnol. Rev.*, vol. 8, no. 1, pp. 562–572, 2019.
[30] A. Bukowczan, E. Hebda, and K. Pielichowski, "The influence of nanoparticles on phase formation and stability of liquid crystals and liquid crystalline polymers," *J. Mol. Liq.*, vol. 321, p. 114849, 2021.
[31] L. Ounoughene, G., Chivas-Joly, C., Longuet, C., Le Bihan, O., Lopez-Cuesta, J. M., & Le Coq, "Evaluation of nanosilica emission in polydimethylsiloxane composite during incineration," *J. Hazard. Mater. 371, 415-422. alcohol. J. Korean Wood Sci. Technol. 51(1)*, pp. 1–13, 2019.
[32] N. Elizondo-Villarreal *et al.*, "Synthesis and Characterization of SiO2 Nanoparticles for Application as Nanoadsorbent to Clean Wastewater," *Coatings*, vol. 14, no. 7. 2024.
[33] J. Gu, X. Cai, Y. Wang, D. Guo, and W. Zeng, "Evaluating the Effect of Nano-SiO(2) on Different Types of Soils: A Multi-Scale Study.," *Int. J. Environ. Res. Public Health*, vol. 19, no. 24, Dec. 2022.
[34] H. Pereira, J. Graça, and J. Rodrigues, "Wood Chemistry in Relation to Quality," *Cheminform*, vol. 35, Nov. 2004.
[35] S. Sankar, N. Kaur, S. Lee, and D. Y. Kim, "Rapid sonochemical synthesis of spherical silica nanoparticles derived from brown rice husk," *Ceram. Int.*, vol. 44, no. 7, pp. 8720–8724, 2018.
[36] I. S. Cahyani, A. Prasetya, H. T. B. M. P., and C. W. Purnomo, "Nanosilica from geothermal sludge using sol-gel method with addition of CTAB surfactants," *AIP Conf. Proc.*, vol. 2391, no. 1, p. 40004, Mar. 2022.
[37] Z. Lu, W. Hu, F. Xie, L. Zhuo, and B. Yang, "Sol–gel synthesis of nanosilica-coated para-aramid fibers and their application in the preparation of paper-based friction materials," *RSC Adv.*, vol. 7, no. 49, pp. 30632–30639, 2017.
[38] C. K. Manchanda, R. Khaiwal, and S. Mor, "Application of sol–gel technique for preparation of nanosilica from coal powered thermal power plant fly ash," *J. Sol-Gel Sci. Technol.*, vol. 83, no. 3, pp. 574–581, 2017.
[39] A. Thuadaij, N., & Nuntiya, "Preparation of nanosilica powder from rice husk ash by precipitation method," *Chiang Mai J. Sci. 35(1)*, pp. 206–211, 2008.
[40] A. Gerasimov, O. Eremina, M. Cherkasova, and S. Dmitriev, "Application of particle-size analysis in various industries," *J. Phys. Conf. Ser.*, vol. 1728, p. 12003, Jan. 2021.
[41] R. Patil and R. Dongre, "Preparation of silica powder from rice husk," *IOSR J. Appl. Chem.*, pp. 26–29, 2014.
[42] B. Lu, Z., Hu, W., Xie, F., Zhuo, L., & Yang, "Sol–gel synthesis of nanosilica-coated para aramid fibers and their application in the preparation of paper-based friction materials," *RSC Adv. 7(49), 30632–30639. https//doi.org/10.1039/C7RA05142E*, 2017.
[43] Z. Cheng, H. Shan, Y. Sun, L. Zhang, H. Jiang, and C. Li, "Evolution mechanism of surface hydroxyl groups of silica during heat treatment," *Appl. Surf. Sci.*, vol. 513, p. 145766, 2020.

[44] P. Nagraik, S. R. Shukla, B. U. Kelkar, and B. N. Paul, "Wood modification with nanoparticles fortified polymeric resins for producing nano-wood composites: a review," *J. Indian Acad. Wood Sci.*, vol. 20, no. 1, pp. 1–11, 2023.

[45] E. Kastner and Y. Perrie, "Particle Size Analysis of Micro and Nanoparticles BT-Analytical Techniques in the Pharmaceutical Sciences.," *Springer New York*, pp. 677–699, 2016.

[46] R. Rahayu, I., Khoerudin, R., Wahyuningtyas, I., Prihatini, E., & Ismail, "Quality Evaluation of Fast-Growing Wood Impregnated with Nano-Silica Synthesized from Betung Bamboo Stems," *J. Sylva Lestari*, pp. 12(3), 684–711, 2024.

[47] N. Karunakaran, G., Suriyaprabha, R., Rajendran, V., & Kannan, "Effect of contact angle, zeta potential and particles size on the in vitro studies of Al2 O3 and SiO2 nanoparticles.," *IET nanobiotechnology*, vol. 9(1), pp. 27–34, 2015.

[48] R. A. Kepekçi, B. Yener İlçe, and S. Demir Kanmazalp, "Chapter 8-Plant-Derived Biomaterials for Wound Healing. In B. T.-S. in N. P. C. Atta-ur-Rahman (Ed.), Elsevier," *Bioact. Nat. Prod.*, 2021.

[49] A. Sikora *et al.*, "A systematic comparison of different techniques to determine the zeta potential of silica nanoparticles in biological medium," *Anal. Methods*, vol. 7, no. 23, pp. 9835–9843, 2015, doi: 10.1039/C5AY02014J.

[50] L. M. Alvarez-Berrios, M. P., Aponte-Reyes, L. M. Aponte-Cruz, and J. L. Loman-Cortes, P., ViveroEscoto, "Effect of The Surface Charge of Silica Nanoparticles on Oil Recovery: Wettability Alteration of Sandstone Cores and Imbibition Experiments.," *Int. Nano Lett.*, vol. 8(3), pp. 181–188, 2018.

[51] A. K. Hamzah, M. H., Saaid, I. M., & Idris, "Particle stability of nano-zinc oxide and nano-silica in sodium silicate solution," *AIP Conf. Proc.*, vol. Vol. 2168, 2019.

[52] W. Liu, C., Wang, X., Qin, L., Li, H., & Liang, "Magnetic coagulation and flocculation of a kaolin suspension using Fe3O4 coated with SiO2," *J. Environ. Chem. Eng.*, vol. 9(5), p. 105980, 2021.

[53] I. Daou, G. Lecomte-Nana, N. Tessier-Doyen, C. Peyratout, M. Gonon, and R. Guinebretière, "Probing the Dehydroxylation of Kaolinite and Halloysite by In Situ High Temperature X-ray Diffraction," *Minerals*, vol. 10, p. 480, May 2020.

[54] V.-C. Niculescu, "Mesoporous Silica Nanoparticles for Bio-Applications," *Front. Mater.*, vol. 7, 2020.

[55] S. M. Khoshnazar, A. Asadi, R. Holghoomi, and A. Abdolmaleki, "Green Synthesis of Silica Nanoparticles/Nanocomposites for Biomedical Applications: A Narraitive Review," *Biochem. (Moscow), Suppl. Ser. B Biomed. Chem.*, vol. 17, no. 2, pp. 41–49, 2023.

[56] J. Hargreaves, "Some considerations related to the use of the Scherrer equation in powder X-ray diffraction as applied to heterogeneous catalysts," *Catal. Struct. React.*, vol. 2, pp. 33–37, Oct. 2016.

[57] C. L. Hobday, S. Krause, S. M. J. Rogge, J. D. Evans, and H. Bunzen, "Perspectives on the Influence of Crystal Size and Morphology on the Properties of Porous Framework Materials," *Front. Chem.*, vol. 9, no. November, pp. 1–10, 2021.

[58] M. Modan and A.-G. Schiopu, "Advantages and Disadvantages of Chemical Methods in the Elaboration of Nanomaterials," vol. 43, Jun. 2020.

[59] H. N. Kim and K. S. Suslick, "The effects of ultrasound on crystals: Sonocrystallization and sonofragmentation," *Crystals*, vol. 8, no. 7, 2018, doi: 10.3390/cryst8070280.

[60] J. E. Arnold and G. M. Day, "Crystal Structure Prediction of Energetic Materials," *Cryst. Growth Des.*, vol. 23, no. 8, pp. 6149–6160, Aug. 2023.

[61] A. Altomare, N. Corriero, C. Cuocci, A. Falcicchio, A. Moliterni, and R. Rizzi, "{\it QUALX2.0}: a qualitative phase analysis software using the freely available database POW_COD," *J. Appl. Crystallogr.*, vol. 48, no. 2, pp. 598–603, Apr. 2015, doi: 10.1107/S1600576715002319.

[62] B. Mysen and P. Richet, "Chapter 5 - Silica," B. Mysen and P. B. T.-S. G. and M. (Second E. Richet, Eds., Elsevier, 2019, pp. 143–183.

[63] J. Bowyer, R. Schmulsky, and J. Haygreen, *Forest Products and Wood Science: An Introduction. 5th Edition.* Ames (USA): Iowa State Press, 2007.

[64] I. S. Rahayu *et al.*, "Impregnation Effect of Synthesized Fe3O4 Nanoparticles on the Jabon Wood's Physical Properties," *Int. J. Recent Technol. Appl. Sci.*, vol. 6, no. 2 SE-Articles, Sep. 2024.